X Encontro Brasileiro sobre Adsorção
27 a 30 de Abril de 2014
Guarujá - SP

CARBOXYLIC ACID RECOVERY FROM AQUEOUS SOLUTIONS BY ACTIVATED CARBON PRODUCED FROM SUGARCANE BAGASSE.

A. Bautista-Carrizosa[1]; E. Suescún-Mathieu[1;] L.Giraldo[2], R.Sierra[1], J.C. Moreno-Piraján[3]

1-Departamento de Ingeniería Química – Universidad de los Andes
Cra. 1 Este 19A-40 – CEP: 111711 – Bogotá D. C. - BOG – Colombia
Telephone: (57-1) 3394949-3095 – Fax: (57-1) 3324334 – Email: rsierra@uniandes.edu.co
1-Departamento de Química – Universidad Nacional de Colombia
Cra. 30 No 43-00 – CEP: 111711 – Bogotá D. C. - BOG – Colombia
Telephone: (57-1) 3394949-3095 – Fax: (57-1) 3324334 – Email: lgiraldogu@uniandes.edu.co
1- Facultad de Ciencias ,Departamento de Química – Universidad de los Andes, Grupo de Investigación en Sólidos Porosos y Calorimetría, Cra. 1 Este 19A-40 – CEP: 111711 – Bogotá D. C. - BOG – Colombia
Telephone: (57-1) 3394949-3095 – Fax: (57-1) 3364300 – Email: jumoreno@uniandes.edu.co

ABSTRACT: This project explores the use of activated carbon (AC) synthesized from sugarcane bagasse (SB) to adsorb volatile carboxylic acids (VCA). Activation was performed by impregnation of SB with 20 and 35% v/v H_3PO_4 (resulting ACA20 and ACA35 respectively) and by impregnation with 30 and 40% v/v $ZnCl_2$ (resulting ACB30 and ACB40 respectively). Since a low adsorption of VCA was expected in acid activated carbons, they were modified with KOH resulting ACA20M and ACA35M. Characterization of the ACs produced showed points of zero charge between 8.4 and 9.2 that favor chemisorption of anions as VCA carboxylates, and essentially microporous carbons. ACB40 showed the highest individual VCA molar adsorption percentages, followed by ACA35M which also showed a highly microporous surface and sites of high adsorption energy on the N_2 adsorption isotherms. Desorption by sonication and heating was performed on ACB40 after acetic acid adsorption, obtaining the highest desorption percentage by sonication.

KEYWORDS: Activated carbon, sugarcane bagasse, chemical activation, volatile carboxylic acids.

1. INTRODUCTION

Within the sugar industry sugarcane stalks undergo a juice extraction process, which results in a fibrous lignocellulosic residue known as bagasse. Sugarcane bagasse (SB) represents about 25% of the sugarcane, and it is primarily intended to replace fossil fuels in industrial operations inside the sugar mills (Ravelo-Ron *et al.*, 2002). In Colombia, this results in a 15% of the overall bagasse as a residue. According to the Statistics Division of the Food and Agriculture Organization of the United Nations (FAOSTAT), in 2011 Colombia was ranked as the thirteenth largest producer of sugarcane in the world, with a production of 22,728,758 tonnes valued at 746,344 thousand dollars. Consequently, Colombia produces approximately 852,328 tonnes per year of SB as a residue. Given that SB shows high availability, low cost, low inorganic matter content, ease of activation, and low degradation upon storage after appropriate drying (Marsh & Rodríguez-Reinoso, 2006), it is of interest to

consider it as a raw material for the generation of value-added products such as AC.

The MixAlco™ process is an emerging advanced biotechnology that transforms any biodegradable feedstock into high-value fuels and chemicals via VCA (Holtzapple *et al.*, 1999) (Nachiappana *et al.*, 2011). However, these acids are obtained in a concentration that does not exceed 20% v/v, thus requiring neutralization and an energy demanding evaporation step in order to concentrate the VCA salts and ensure a high conversion in subsequent stages (López, 2013). Aiming to reduce operating costs associated with MixAlco™ process energy requirements, and to take advantage of readily available agro-industrial residues, the present study focused on the synthesis and characterization of activated carbons produced from SB, which were used for the adsorption of VCA. The carbons were chemically activated both in acidic and basic media, and they were characterized to determine their properties. Additionally, desorption of the adsorbed VCA through sonication and heating was explored.

2. METHODS

2.1. AC Synthesis

The SB was placed in a MERMMET UFB 700 oven at 45 °C for two weeks. After reaching a moisture content lower than 10%, the SB was grinded and sieved with Tyler meshes. 50 g of the recovered fraction, corresponding to -20/+80, were taken for each one of the four activations. Impregnations were performed with 20% v/v H_3PO_4, 35% v/v H_3PO_4, 30% v/v $ZnCl_2$, and 40% v/v $ZnCl_2$, and the corresponding AC samples were named ACA20, ACA35, ACB40, and ACB30. The impregnated samples were placed in a LINDBERG/BLUE Gravity One oven at 80°C for three days, and then placed in a Carbolite 1009 furnace at 850°C for 4 hours, using a temperature ramp of 10°C min-1 in an inert atmosphere (N_2). In order to remove the zinc salts, 50 mL of 0.1 M HCl were added to the resulting ACB samples and stirred at 100 rpm and 150 °C until boiling. ACB samples were filtered and then, all AC samples were washed with deionized water in a Soxhlet until reaching a constant pH. Because the adsorption of VCA on the ACA samples was expected to be low, their surface was modified by adding 100 mL of KOH at 40% v/v to 10 grams of ACA and placing the samples in an incubator at 70 °C for two hours. The samples were agitated in a shaker at 35 °C for 24 h, and then washed with deionized water in a Soxhlet until reaching a constant pH. The modified samples were named ACA20M and ACA35M respectively. Finally, the four AC samples were dried in a MERMMET UFB 500 oven at 80 °C for 24 hours.

2.2. AC Characterization

For the Boehm method 50 mL of 0.1 N solutions of $NaHCO_3$, Na_2CO_3, NaOH and HCl were prepared and standarized. 0.1 g of AC was suspended in these solutions for six days, and then they were titrated to determine the surface functional groups (Boehm, 2002). For the point of zero charge (PZC) different amounts of the AC samples, ranging from 0 to 0.6 g, were weighed and placed in a 30 mL flask with 10 mL of a 0.1 M NaCl solution. The bottles were capped and stirred at 25 °C for 3 days, and then the pH of each solution was measured (Chan *et al.*, 2011). The measurements of the volume of N_2 adsorbed on the AC surface, were taken in an Autosorb Quantachrome Model 3B varying the N_2 relative pressure at 77 K.

2.3. VCA Adsorption

To study the capability of the AC samples to adsorb individual VCA, 100 mL of the following 20% v/v solutions in water were prepared: Acetic acid, propanoic acid, and butyric acid. 1 g of AC was added to each one of the three acid solutions, and then an aliquot of the solution was taken every 12 hours during a 3 day period. These aliquots were analyzed through gas chromatography to determine the adsorption capacity, and this procedure was applied to each one of the four AC samples (López, 2013).

In order to have a more realistic approach to the adsorption performance of the AC samples inside the MixAlco™ countercurrent fermentation reactors, in which VCA are mixed at different concentrations primarily with water, a 100 mL solution in water containing acetic acid at 16% v/v, propionic acid at 2% v/v and butyric acid at 2% v/v was prepared to conduct a competitive adsorption test. Then, the same sampling and analysis procedure as in individual adsorption was applied for each one of the four AC samples (López, 2013).

2.4. Desorption Tests

Four different desorption tests were performed for the AC sample that showed the highest levels of VCA adsorption. The implemented techniques were sonication (S), heating (H), sonication followed by heating, (S+H) and, finally, heating followed by sonication (H+S). Sonication was performed using a Sonics & Materials Inc. VCX-756 tip sonicator, which operates for 20 seconds and stops for 40 seconds per minute. It was used for 35 min on a falcon containing 1 g of AC and 5 mL of deionized water. Heating was carried out in a Barnstead/Labline SHKE7000 incubator at 60 °C for 24 h using the same amounts of AC and deionized water in a closed flask. An aliquot of the resulting solutions was taken, filtrated, and submitted to a chromatographic analysis in order to determine de amount of desorbed VCA.

2.5. Scanning Electron Microscopy (SEM)

It was performed using a JEOL JSM-649OLV SEM, to reveal the morphology and superficial structures of the ACs and the SB. It is a useful tool to observe the particle surface and the extension of the pores (Marsh & Rodríguez-Reinoso, 2006).

3. RESULTS AND DISCUSSION

3.1. Surface Chemistry

The surface chemistry of the AC samples was analyzed by the Boehm method.

Table 1 shows the surface functional groups of the AC samples in relation to the values of pH_{PZC}. These results show that activating the SB with $ZnCl_2$ as a basic impregnating agent or modifying the H_3PO_4 activated carbons with KOH, leads to an enrichment in surface basic groups and, therefore, increases the pH_{PZC}. At a pH lower than these pH_{PZC} values the carbons surface will exhibit a net positive charge, promoting the chemisorption of anions such as VCA carboxylates to produce VCA salts.

Table 1. Surface functional groups concentration for SB and AC samples, obtained by the Boehm method, compared to the pH_{PZC}. Concentrations are shown in µmol per gram of AC.

Sample	pH_{PZC}	Functional groups concentration (µmol g^{-1})				
		Carboxyl	Lactonic	Fenolic	Acid	Basic
SB	8.3	68.6	29.4	107.8	205.8	29.4
ACB30	8.4	49.0	19.6	93.1	161.7	181.3
ACB40	8.7	39.2	19.6	83.3	142.1	196.0
ACA20M	8.5	34.3	14.7	78.4	127.4	220.5
ACA35M	9.2	19.6	9.8	68.6	98.0	269.5

Given that all the pH_{PZC} obtained are basic, and that a pH lower than 7 will be obtained at the end of the stage of acidogenic fermentation of the MixAlco™ process, VCA carboxylates adsorption will be favored. Figure 1 shows a schematic representation of the chemisorption mechanism occurring during VCA adsorption tests.

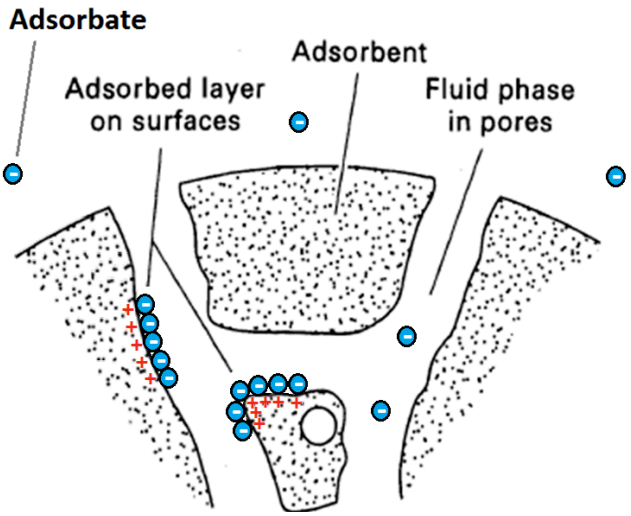

Figure 1. Chemisorption of VCA carboxylates on AC. Adapted from Seader and Henley (2006).

3.2. N_2 Adsorption Isotherms

The nitrogen adsorption and desorption isotherms for the four AC samples, are presented in Figure 2. Regardless of the activation procedure, the data obtained for all AC samples adjust to a type I isotherm, which is exclusive for completely microporous solids. The adsorbed amount of adsorbate increases with the relative pressure, until reaching a final value corresponding to the total coverage of the surface with an adsorbate monolayer.

The gradients of the initial part of the isotherm, at P/P_0 values from zero to about 0.05, are an indicative of the microporosity dimensions, so the steeper the gradient, the narrower the micropores. Based on this, ACA35M followed by ACA20M have the narrower pores among the studied AC samples. The initial part of the isotherm, at values of $P/P_0 << 0.001$, indicates the presence of sites of high adsorption energy (Marsh & Rodríguez-Reinoso, 2006), which are slightly more visible for the ACA35M isotherms. Given that activated carbons in industrial applications need to adsorb at low relative pressures in gas phase, and taking into account the highly microporous surface, small pore size, and sites of high adsorption energy of ACA35M, it is profiled as a good option for industrial applications.

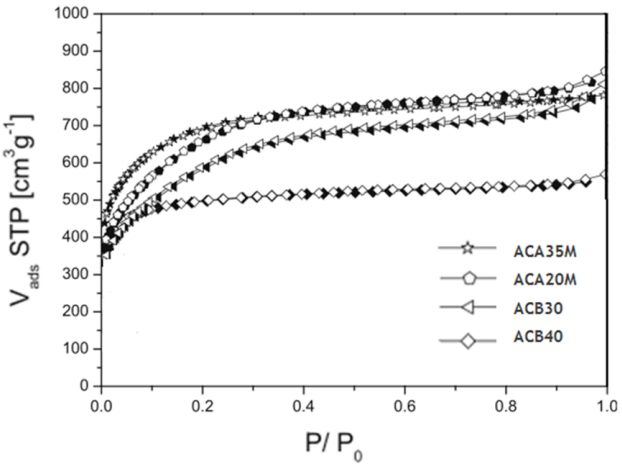

Figure 2. Adsorption and desorption isotherms of nitrogen at 77 K for the four AC samples. V_{ads} represents the volume of adsorbate (N_2) adsorbed per gram of AC, and P/P_0 is the relative pressure at the gas saturation pressure.

Figure 3 shows the pore distribution of the AC samples.

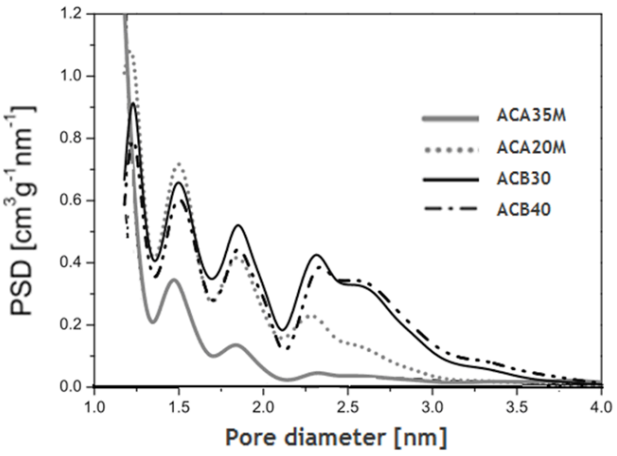

Figure 3. Pore size distribution (PSD) obtained by applying the DFT theory to the data of N_2 adsorption isotherms at 77K

The four AC samples have primarily a pore size distribution below 2 nm, so the ACs produced in this study are mainly microporous, as it was previously stated. Likewise, the presence of mesopores is observed, but in such a small degree that adsorption in mesopores is neglected. Instead, mesopores may be considered the entrance to the micropores, where the bulk of the adsorption takes place. ACA35M exhibited the largest microporous surface area, followed by ACA20M, ACB30 and ACB40 in decreasing order. Numerical data regarding the textural parameters of the AC

obtained from N_2 adsorption isotherms, are shown in Table 2.

Table 2. Textural parameters of the activated carbons, prepared from N_2 isotherms at 77 K.

Sample	S_{micro} ($m^2\ g^{-1}$)	S_{meso} ($m^2\ g^{-1}$)	V_{total} ($cm^3\ g^{-1}$)	$V_{microDFT}$ ($cm^3\ g^{-1}$)
ACA20M	1400	350	0.442	0.289
ACA35M	1455	220	0.413	0.275
ACB30	1345	55	0.386	0.042
ACB40	1055	245	0.321	0.132

3.3. VCA Adsorption

As seen in Table 3, the maximum removal of VCA was obtained in individual adsorption since the higher the initial concentration of a single VCA, the higher the percentage thereof adsorbed. The lower percentage of adsorption obtained for the competitive tests, can also be explained by interactions between molecules and ions in the solution that compete for adsorption sites. ACB40 showed the highest individual VCA adsorption percentages. However, individual adsorption percentages for the other AC samples are considerably similar. It is also noticed a higher adsorption percentage by ACB in comparison to ACA modified with KOH. However, by comparing these results with those obtained from the N_2 adsorption isotherms, ACA have a higher volume of micropores than the ACB and should therefore have a greater capacity for removing VCA from aqueous solutions. This may be explained by the differences in surface functional groups, which promote a higher affinity between ACB and VCA than between ACA and VCA. Another possible explanation is an incomplete Soxhlet washing of ACA after modification, so that the porous surface may be covered with potassium phosphates resulting from the reaction between the impregnating agent (H_3PO_4) and the modifying agent (KOH), thus obstructing the adsorption of VCA but allowing the smaller molecules of N_2 to enter the micropores. In all cases, acetic acid was the adsorbate with the highest adsorption percentages due to its smaller length (approximately 0.3 nm) in comparison to propionic acid (approximately 0.4 nm) and butyric acid (approximately 0.5 nm) (Sutton, 1965). This allowed acetic acid molecules to easily move through the micropores and to fill them in a more compact way than the other two adsorbates.

Table 3. Molar adsorption percentages of each AC sample for the individual and competitive adsorption tests.

	Individual adsorption test			Competitive adsorption test		
Sample	Acetic acid	Propionic acid	Butyric acid	Acetic acid	Propionic acid	Butyric acid
ACB40	60%	48%	21%	25%	2%	10%
ACB30	56%	48%	19%	26%	5%	6%
ACA35M	54%	46%	10%	16%	12%	5%
ACA20M	53%	44%	10%	19%	9%	9%

3.4. Desorption Tests

Given that ACB40 exhibited the highest acetic acid adsorption percentage, the sample designated as ACB40A (ACB40 after acetic acid adsorption), was used for the desorption tests consisting on four combinations of sonication and heating: Sonication (S), heating (H), sonication followed by heating (S+H), and heating followed by sonication (H+S). The corresponding desorbed samples were named ACB40AS, ACB40AH, ACB40AS+H, ACB40AH+S. Figure 4 shows the percentage of acetic acid desorption for the four desorption tests applied.

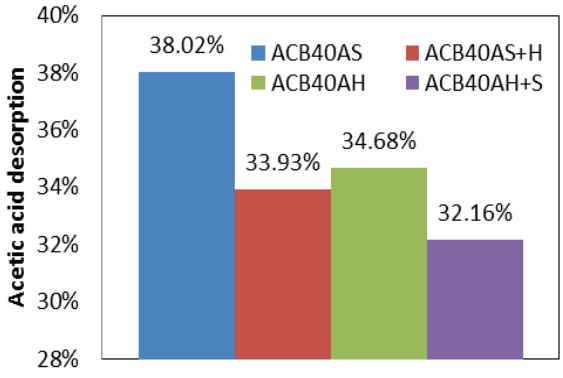

Figure 4. Acetic acid desorption percentage using different combinations of sonication (S) and heating (H) on ACB40A.

As shown in the graph, the highest VCA desorption percentage was obtained by sonication. A feasible explanation is that heating caused the volatilization of the desorbed VCA, provoking a loss of these when the container was opened to take aliquots. This would also explain why heating and subsequent sonication (H+S) showed the lowest VCA desorption percentage, given that sonication required the flask containing the warm sample to stay open. During sonication, ultrasonic waves generate vibrations in the adsorbent and the adsorbate provoking the desorption of the most weakly bound particles, such as those adsorbed by physisorption. However, since most of the VCA is adsorbed by chemisorption, the vibration does not have sufficient energy to break the acid-base bonds in the surface of the AC.

3.5. Scanning Electron Microscopy (SEM)

Micrographs obtained by SEM are shown in Figure 5, where the change in SB superficial texture and porosity after activation and modification, is evidenced. The micrograph on Figure 5.a shows the layered lignocellulosic structure of SB, where small pores related to the circulatory system of the sugarcane can be seen. The diameter of these pores is of approximately 1 µm, and they can also be seen in Figure 5.g and 5.h. The cavities and fractures are due to the rupture caused by SB pretreatment (Chen *et al.*, 2011). Figure 5.b, 5.e and 5.f show the irregular structure of ACB40 powder particles, which confers it an elevated surface area. In Figure 5.b to 5.f, the porous structure of the AC samples can be seen. The porosity created by $ZnCl_2$ is due to the spaces left by this salt after washing given that it behaves as a template; subsequently, the uniform size of the micropores is due to the small size of the $ZnCl_2$ molecule or its hydrates. This does not happen for H_3PO_4 because there are no phosphoric acid molecules, but a mixture of molecules from the small H_3PO_4 to $H_{13}P_{11}O_{34}$; this leads to heterogeneity in the microporosity of ACA samples.

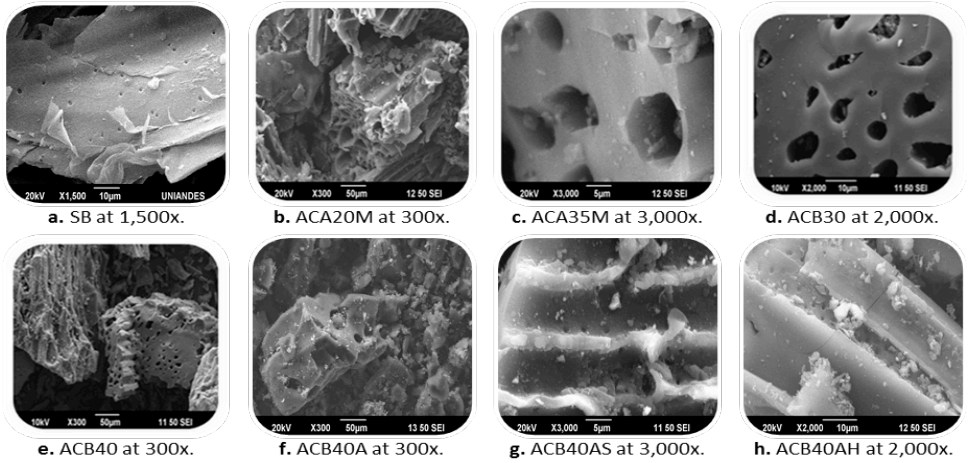

Figure 5. SEM images for the SB and selected AC samples.

In Figure 5**¡Error! No se encuentra el origen de la referencia.**.f small white dots can be seen on the ACB40A surface, which can be attributed to the carboxylic salts that form on the surface of the AC as a result of chemisorption of the acetic acid. On **¡Error! No se encuentra el origen de la referencia.**.g and 5.h, corresponding to the ACB40A samples with the best desorption results, salts are still observed on the carbon

surface, being necessary to employ new desorption techniques to obtain better results. The presence of these salts on the ACA samples prior to adsorption (see Figure 5.b and 5.c) can be explained by the reaction between H_3PO_4 and KOH to produce potassium phosphates, which could have remained on the ACA due to an incomplete Soxhlet washing after modification. The presence of salts on ACB surface may be also due to an incomplete wash of the samples. However, it is of importance to note that the presence of salts on the AC samples before adsorption is low.

4. CONCLUSIONS

Activating the SB with $ZnCl_2$ as a basic impregnating agent or modifying the H_3PO_4 activated carbons with KOH, leads to an enrichment in surface basic groups and, therefore, increases the pH_{PZC}. Given that all the pH_{PZC} obtained are basic, and that a pH lower than 7 will be obtained at the end of the stage of acidogenic fermentation of the MixAlco™ process, VCA carboxylates adsorption on the ACs will be favored.

SEM micrographs show the irregular and porous structure of AC powder particles, which confers them an elevated surface area. In the micrographs corresponding to the AC samples with the best desorption results (ACB40AS and ACB40AH), salts formed by chemisorption of VCA are still observed in the carbon surface, being necessary to employ new desorption techniques to obtain better results.

N_2 adsorption isotherms obtained for all AC samples, regardless of the activation procedure, adjust to a type I isotherm, which is exclusive for completely microporous solids, where the absorption takes place in a monolayer. The four AC samples have primarily a pore size distribution below 2 nm, so the AC samples produced in this study are mainly microporous. ACA35M exhibited the largest microporous surface area, followed by ACA20M, ACB30 and ACB40 in decreasing order. ACA35M is profiled as a good option for industrial applications in gas phase, due to its highly microporous surface and its sites of high adsorption energy.

ACB40 showed the highest individual VCA adsorption percentages. It was also noticed a higher VCA adsorption percentage by ACB in comparison to the more microporous ACA modified with KOH, which may be due to an incomplete washing of the ACA after modification, so that the porous surface may be covered with potassium phosphate (K_3PO_4) resulting from the reaction between the impregnating agent (H_3PO_4) and the modifying agent (KOH), thus impeding the adsorption of VCA.

The highest VCA desorption percentage was obtained by sonication, while heating seemed to provoke the loss of VCA by volatilization. It is suggested for a future work to investigate further desorption methods that allow the breakage of the bonds formed between the adsorbate and the adsorbent, without generating loss of the desorbed species.

5. REFERENCES

BOEHM, H. P. (2002). Surface Oxides on Carbon and Their Analysis: A Critical Assessment. *Carbon, 40*(2), 145-149.

CHAN, O. S., CHEUNG, W. H., & MCKAY, G. (2011). Preparation and Characterization of Demineralized Tire Derived Activated Carbon. *49*, 4674-4687.

CHEN, W. H., TU, Y. J., & SHEEN, H. K. (2011). Disruption of Sugarcane Bagasse Lignocellulosic Structure by Means of Dilute Sulfuric Acid Pretreatment With Microwave-Assisted Heating. *Applied Energy, 88*(8), 2726-2734.

HOLTZAPPLE, M. T., DAVISON, R. R., ROSS, M. K., ALDRETT-LEE, S., NAGWANI, M., LEE, C. M., LEE, C., ADELSON, S., KAAR, W., GASKIN, D., SHIRAGE, H., CHANG, N. S., CHANG, V. S., LOESCHER, M. E. (1999). Biomass Conversion To Mixed Alcohol Fuels Using the MixAlco Process. *Appl. Biochem. Biotechnol., 79*(1-3), 609-631. Retrieved 2013

LÓPEZ, C. (2013). *Adsorción de ácidos carboxílicos de cadena corta sobre carbón activado: Estudio en una reacción de esterificación.* Universidad de los Andes, BA thesis, Departamento de Ingeniería Química, Bogotá.

MARSH, H., & RODRÍGUEZ-REINOSO, F. (2006). *Activated Carbon.* Oxford: Elsevier.

NACHIAPPANA, B., FU, Z., & HOLTZAPPLE, M. T. (2011). Ammonium Carboxylate Production from Sugarcane Trash Using Long-Term Air-Lime Pretreatment Followed by Mixed-Culture Fermentation. *Bioresource Technology, 102*(5), 4210–421.

RAVELO-RON, D., BERMÚDEZ-SAVÓN, R. C., VALIÑO-CABRERA, E., & PÉREZ-PARDO, J. L. (2002). Fermentación del bagazo de caña de azúcar en un biorreactor a escala de laboratorio. *Tecnología química, 22*(2), 32-40.

SEADER, J. D., & HENLEY, E. J. (2006). *Separation Process Principles* (2 ed.). EE.UU.: John Wiley & Sons, Inc.

SUTTON, L. E. (1965). *Tables of Interatomic Distances and Configuration in Molecules ad Ions. Suplement 1956-1959.* London: The Chemical Society.